DOI: 10.21062/mft.2024.064 http://www.journalmt.com

Study on Multi-Objective Optimization of Milling Process of Powder Metallurgy Titanium Aluminum Alloys

Wenbing Tian (0000-0003-3448-8035)[1,2], Wenhu Wang[1,2], Yuanbin Wang (0000-0002-9988-6790)[1,2], Shengguo Zhang (0009-0006-6978-7608)[1,2]
[1]Key Laboratory of High Performance Manufacturing for Aero Engine, Ministry of Industry and Information Technology, School of Mechanical Engineering, Northwestern Polytechnical University, Xi'an 710072, Shaanxi, PR China
[2]Engineering Research Center of Advanced Manufacturing Technology for Aero Engine, Ministry of Education, School of Mechanical Engineering, Northwestern Polytechnical University, Xi'an 710072, Shaanxi, PR China
*Corresponding author (W. Tian), e-mail: twb_npu@163.com

Currently, there is a demand in the aerospace industry for a more effective and non-invasive milling technique for powder metallurgy γ-TiAl alloys. The primary objective of this research is to examine the surface milling process of γ-TiAl alloys generated by powder metallurgy. The primary objective of this study is to examine the impact of process parameters on the surface roughness and cutting force of alloys, with the aim of optimizing both surface roughness and cutting force. The response surface method was implemented to examine the milling process, and the NSGA-II algorithm was employed to optimise surface roughness, cutting force, and material removal rate (MRR). The findings indicate that the cutting depth exerts a significant impact on both the surface morphology and surface roughness. The available data indicates a clear correlation between the depth of cutting and the rate of feed, as well as the resulting assessment of surface roughness. Nevertheless, the first rise in cutting speed is associated with a subsequent increase in surface roughness, followed by a subsequent drop of a lesser magnitude. A minimal threshold for surface roughness has been established at 0.203μm. The cutting speed exerts the primary impact on the cutting force. There exists a positive link between the cutting force value and both the cutting depth and feed speed, as the cutting force value has a positive correlation with the incremental changes in these variables. Nevertheless, the relationship between cutting force and the observed trend is non-linear, exhibiting an initial decrease followed by a rise when cutting force is augmented. The minimal cutting force necessary was quantified as 112.3 N. Subsequently, a regression analysis was employed to develop a correlation model between surface roughness and cutting force and machining parameters. The confirmation of the coefficients' validity in the model was achieved via the utilisation of analysis of variance (ANOVA) and residual analysis. The main goal of developing a machining parameter optimisation model is to limit surface roughness and cutting force, thereby improving operational efficiency. The NSGA-II method is utilised to tackle the problem of multi-objective optimisation, leading to the attainment of the optimal parameter solution. The purpose of the verification test is to evaluate the precision of the forecasts generated by the optimised model. The work holds importance in its analysis and juxtaposition of diverse processing factors, alongside the use of multi-objective optimization methodologies.

Keywords: Powder metallurgy γ-TiAl alloy, Cutting force, Surface roughness, Multi-objective optimization

1 Introduction

The γ-TiAl alloys have advantageous features such as high strength, low density, high resistance to creep, and effective antioxidant properties. Operating in complicated working circumstances for extended periods, particularly in severe environments characterised by high temperature oxidation, exhibits notable performance advancement. Potential materials for high-temperature applications include titanium alloys and nickel-based alloys. At now, γ-TiAl alloys are recognized for their exceptional specific strength and have been successfully employed as a viable substitute for high-temperature nickel-based alloys, particularly at temperatures approximately equal to 750°C. This replace has the benefit of attaining a decrease in weight of around 50% [1–3].

The aerospace industry faces limitations in the widespread adoption of γ-TiAl due to its expensive material costs and the difficulties involved in achieving precise processing methods, despite its outstanding mechanical and thermodynamic properties. γ-TiAl alloys have limited toughness, reduced thermal conductivity, poor fracture resistance, pronounced cracking,

and a propensity for reacting with tool materials. The primary constraints associated with γ-TiAl encompass surface micro-cracks, material pull-out, edge defect, and heightened surface roughness. The presence of these imperfections can serve as nucleation sites for the advancement of fractures, ultimately resulting in the failure of the object [4]. Furthermore, the diminished surface integrity of γ-TiAl components have a detrimental impact on the fatigue and creep properties of the blades, hence constraining their extensive utilisation across many technical domains.

Previous studies have solely yielded some qualitative experimental findings pertaining to the integrity of the casting surface of γ-TiAl. However, it has been observed that alloys based on γ-TiAl exhibit suboptimal casting qualities and are susceptible to the occurrence of casting defects. Powder metallurgy is a highly advantageous technique for the production of TiAl-based alloys, since it effectively eliminates issues such as macro-compositional segregation, porosity, and shrinkage. Consequently, it has become one of the primary methods employed in the manufacture of these alloys [5]. The advancements in pre-alloyed powder and elemental powder preparation techniques have led to enhancements in the tensile strength, elongation, and oxidation resistance of powder metallurgy γ-TiAl alloys. Additionally, it may be inferred that the machinability of powder metallurgy titanium aluminium alloy is inferior to that of casting titanium aluminium alloy. Currently, there is a limited amount of literature available regarding the machining of powder metallurgy γ-TiAl alloys. Therefore, there is a pressing need to undertake comprehensive investigations into the machining processes of powder metallurgy titanium aluminium alloy [6].

In recent years, there have been a considerable body of research conducted on the manufacturing of γ-TiAl. The study conducted by Priarone et al. [7] aimed to enhance the machinability of EBM sintered Ti-48Al-2Cr-2Nb by the adjustment of tool geometry parameters using the tool post-treatment procedure. The findings of the study indicated that a reduction in the radial rake angle and an increase in the edge radius were associated with improved tool longevity. Furthermore, the findings of their study indicated that the tool longevity of AlSiTiN-coated tools exhibited a higher level of performance compared to that of CrAlSiN-coated tools. In a separate study, Priarone et al. [8] conducted an investigation into the impact of lubrication strategy on tool longevity during the processes of Ti-48Al-2Cr-2Nb intermetallic alloys. The investigation focused on analyzing the impact of lubrication technique on both surface quality and tool wear. The results of the study suggest that wet cutting demonstrated a decrease in surface roughness and tool wear when compared to dry cutting. Specifically, the use of micro lubrication (MQL) proved to be the optimal approach for dry cutting. The investigation of the effects of lubrication and cooling types on γ-TiAl alloys was conducted in separate studies by Kolahdouz et al. [9] and Rotella et al. [10]. The study revealed that MQL had specific characteristics. Achieving a decrease in work hardening and surface roughness is possible. The study conducted by Settineri et al. [11] examined the impact of cooling and lubrication parameters on three distinct γ-TiAl alloys, namely Ti-45Al-2Nb-2 Mn-0.8 vol. % TiB2XD, Ti-48Al-2Cr-2Nb, and Ti-43.5Al-4Nb-1Mo-0.1B). The machinability of specimens was investigated through milling and turning experiments. The objective of this study was to evaluate the effects of different alloying components on the mechanical characteristics of the materials and ascertain their influence on machinability. The findings revealed that Ti-48Al-2Cr-2Nb exhibited the highest ease of machinability, whereas Ti-45Al-2Nb-2Mn-0.8 vol. % TiB2XD) demonstrated a lower level of machinability, however it demonstrated comparatively lower surface roughness. Beranoagirre et al. [12] conducted a comprehensive series of milling experiments to investigate the correlation between tool wear and feed rate and cutting speed. Furthermore, a comparative analysis was conducted on the chip morphology of the three materials, as well as the correlation between material removal and tool wear. It was determined that for tungsten carbide tools coated with (AlTi)N, the optimal cutting speed falls within the range of 50 to 70 $m.min^{-1}$, while the recommended feed rate ranges from 0.05 to 0.06 mm. The present study provides a summary of the reference tool life of the MoCuSi extrusion alloy under specific cutting conditions, namely a cutting speed of 50 $m.min^{-1}$ and a feed rate of 0.05 $mm.z^{-1}$. Hood et al. [13] conducted a study in which they utilised an AlTiN-coated WC ball end mill to perform slot milling on a Ti-45Al-2Nb-2Mn-0.8 vol. % TiB2 material. The objective of their research was to investigate the impact of process parameters on both tool wear and surface integrity. Mantle et al. [14] conducted a series of milling tests on a Ti-45A-2Nb-2Mn-0.8 vol. % TiB2 alloy. The objective of these investigations was to examine the influence of different process parameters on the surface integrity of the material. To do this, WC ball end mills were employed. The findings of the study indicated the presence of several flaws, including material pullout, fracture, smearing, and lamellar deformation, on the surface of the workpiece. Additionally, the measured surface roughness values generally fell below 1.5μm. Hood et al. [15] observed the occurrence of material pullout during the high-speed milling of γ-TiAl alloys. They further noted that both material pullout and tool wear exhibited an upward trend when the cutting speed was raised. Ge et al. [16] conducted an

investigation of the milling effectiveness of γ-TiAl alloy throughout a spectrum of velocities, namely ranging from 60 to 240 m.min^{-1}. The testing results demonstrate that the surface roughness consistently stayed below Ra0.44μm throughout all evaluated cutting speeds, even in instances where the tool wear reached VB0.2 mm. The milling force shown a little elevation when the cutting speed was augmented. but it shown a more pronounced increase with the rise in tooth flank wear value, particularly for the Fy component.

Multiple studies have demonstrated that the implementation of plastic processing techniques during the machining of brittle materials may effectively mitigate surface and subsurface damage as well as micro-cracking of the material [17–19]. Moreover, it should be noted that γ-TiAl exhibits brittleness as a material characteristic. Consequently, while using bigger depths of cut and feed rates during cutting processes, the cutting force tends to escalate. This rise in cutting force can result in brittle fracture occurrences, mostly caused by internal dislocations within the material. Such brittle fractures manifest when the cutting force surpasses the tensile limit of the γ-TiAl material. Reducing the feed rate and depth of cut have been seen to facilitate the plastic deformation of the material, resulting in an overall improvement in surface integrity. The researchers noted that an escalation in cutting speed resulted in a corresponding rise in cutting temperature, which subsequently caused the material to soften [20,21]. Hence, it is plausible to adopt a strategy of elevating the cutting speed while concurrently reducing the feed rate and cutting depth in order to execute plastic processing and attain desirable outcomes with regards to surface roughness and cutting force.

In this work, a comprehensive factorial design was employed to conduct milling experiments. The design consisted of three factors, each with four levels, resulting in a total of twelve tests. The objective was to systematically investigate the impact of cutting parameters on the surface roughness and cutting forces of γ-TiAl. The purpose of this study was to emphasise the potential impact of alterations in process parameters, either individually or in combination. Then, response surface milling experiments were designed to evaluate the milling process and empirical regression equations for surface roughness and cutting force were obtained. Finally, the multi-objective optimization of process parameters for surface roughness, cutting force and material removal rate was carried out in combination with NSGA-II algorithm.

2 Experimental material and process

2.1 Experimental materials

The experimental trials utilised a γ-TiAl alloys (Ti-45Al-2Cr-2Nb-0.8% TiB_2), which was developed by Sino-Euro Materials Technologies of Xi'an Co. Ltd.γ-TiAl was prepared through powder preparation, powder sintering, forming process, heat treatment and other processes. To create an orientated lamellar structure internally, hot isostatic pressing (HIP) was combined with conventional heat treatment. As can be observed in Fig. 1, the lamellar layer's length was around 30–100 μm. Table 1 displays the principal chemical components of the substance, while Table 2 (date supplied by SEMT) displays the mechanical characteristics.

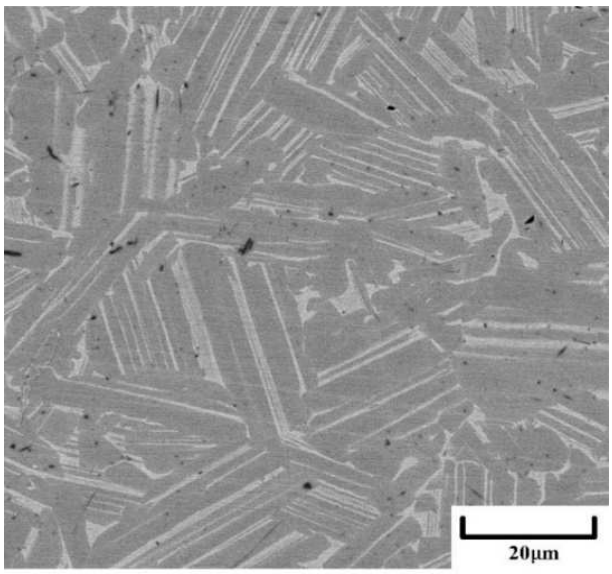

Fig. 1 *SEM of powder metallurgy γ-TiAl alloys*

Tab. 1 *Nominal and measured components of powder metallurgy γ-TiAl alloys*

Elements	Al	Nb	Cr	B	O	C	Ti
Nominal	45	2	2	0.8	-	-	50
Measured	45	1.9	2.33	0.93	0.034	0.0052	49

Tab. 2 *Mechanical properties of powder metallurgy γ-TiAl alloys*

Mechanical properties	Temperature [°C]	
	25	650
Yield strength [MPa]	500	380
Tensile strength [MPa]	650	620
Hardness [HRC]	40	
Tensile rate [%]	1.5	3

2.2 Experimental equipment

The sample size is 70mm × 25mm × 10mm, the experimental machine is VMC-850 vertical milling machine, select ϕ8mm carbide flat-bottomed milling cutter, with the number of teeth N=4, the helix angle of 40 °, and the milling method is forward milling. The whole experimental process is cooled by cooling lubricating oil. The milling results are measured by the probe contact surface measuring instrument Mar-SurfXT20 for the two-dimensional roughness of the workpiece milling surface, and the surface roughness is measured along the feed direction and the vertical feed direction respectively. Select 10 points from the machined surface of each workpiece and take the average value as the measurement value of the workpiece roughness. The cutting force test employed a force measuring equipment manufactured by Kistler, consisting of a Kistler 9257B dynamometer, a Kistler 5080A charge amplifier, and a Kistler 5697A data collector. In order to mitigate the influence of tool wear on cutting force, the cutting forces in the X, Y, and Z axes were integrated during the first stationary stage of cutting.

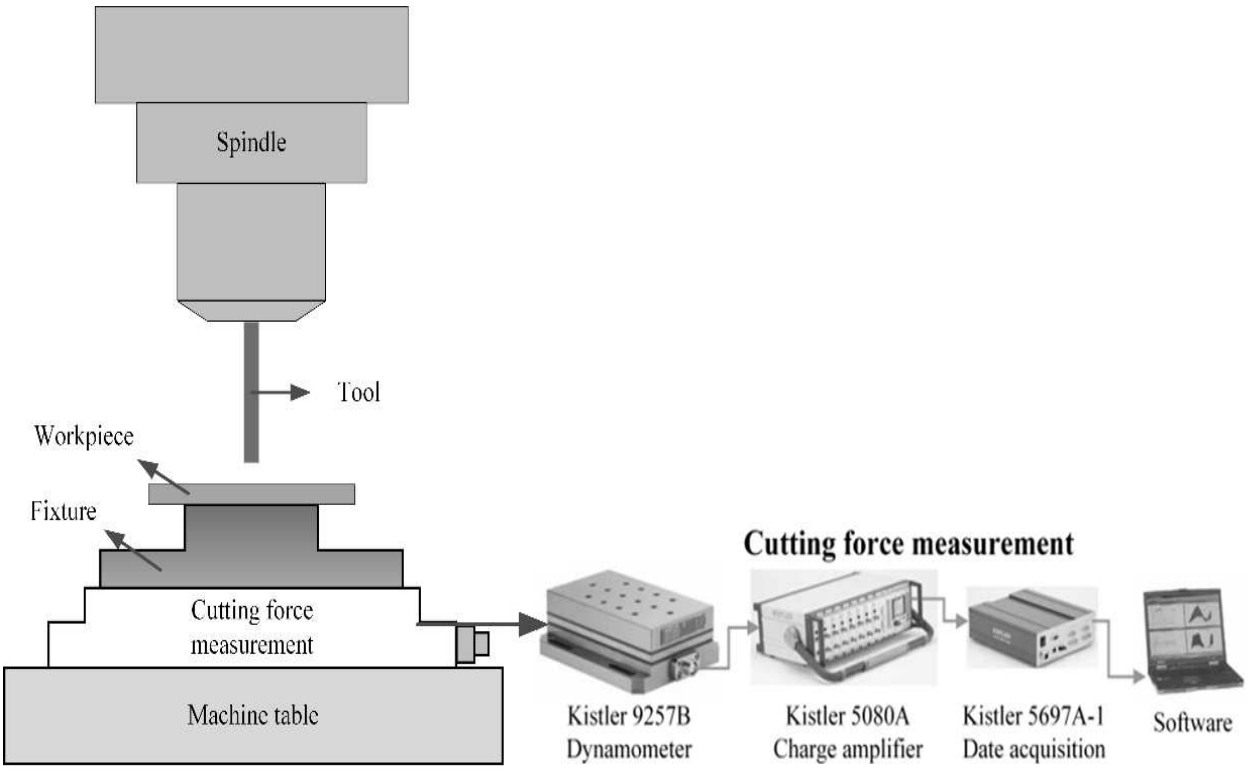

Fig. 2 *Experimental setup*

2.3 Experimental processes and parameters

In order to examine the impacts of alterations to the process parameters, a comprehensive factorial design and orthogonal design were employed in the milling experiments. This design consisted of three factors, four levels, and a total of twelve tests, allowing for the identification and evaluation of the individual or combined effects of these modifications. In order to ensure consistency in the initial cutting conditions, a fresh tool was employed for each sample. Additionally, the single-factor experiment was replicated three times to mitigate the influence of random variables on the experimental results. The range of cutting parameters was determined by combining the comments of the material producer with the findings of multiple trial cutting experiments. The factorial design trial settings and outcomes were established for the thorough consideration of surface quality and cutting force, as shown in Table 3. The specifications and findings of the orthogonal design experiment were established, as seen in Table 4. The investigators utilized a single-factor experimental design to investigate the influence of specific process parameters on the cutting force and surface roughness of γ-TiAl. The experimental setup involved adjusting the cutting width to 7 mm, followed by systematically altering the cutting speed (n_s, m.min^{-1}), cutting depth (a_p, mm) and feed rate (f_z, mm.z^{-1}), to investigate the impact of these cutting parameters on surface roughness, and cutting force. The parameters for cutting utilized in the experimental trials are outlined in Table 5.

Tab. 3 *Experimental results of factorial design for Ra, Sa and F*

No	n_s [m.min^{-1}]	f_z [mm.z^{-1}]	a_p [mm]	Ra [μm]	Sa [μm]	F [N]
1	25.12	0.005	0.1	0.170	0.244	151.9
2	50.24			0.188	0.285	145.3
3	75.36			0.224	0.338	126.8
4	100.48			0.226	0.334	237.7
5	50.24	0.005	0.1	0.188	0.285	151.9
6		0.01		0.202	0.282	171.9
7		0.015		0.220	0.311	198.02
8		0.02		0.379	0.479	227.7
9	50.24	0.005	0.05	0.185	0.268	112.3
10			0.1	0.188	0.285	151.9
11			0.15	0.187	0.283	164.3
12			0.2	0.209	0.320	176.2

Tab. 4 *Experimental results of orthogonal design for Ra, and F*

No	n_s[m.min^{-1}]	f_z[mm.z^{-1}]	a_p[mm]	Ra[μm]	F [N]
1	25.12	0.02	0.125	0.378	189.9
2	25.12	0.005	0.125	0.252	168.8
3	25.12	0.0125	0.05	0.305	132.2
4	25.12	0.0125	0.2	0.312	198.2
5	62.8	0.02	0.2	0.406	212.7
6	62.8	0.0125	0.125	0.346	232.65
7	62.8	0.02	0.05	0.357	201.2
8	62.8	0.005	0.05	0.246	129.6
9	62.8	0.005	0.2	0.286	185.4
10	100.48	0.0125	0.2	0.377	266.3
11	100.48	0.0125	0.05	0.297	228.9
12	100.48	0.005	0.125	0.240	252.38
13	100.48	0.02	0.125	0.383	284.1

Tab. 5 *Experiment cutting parameters*

Test	n_s[m.min^{-1}]	f_z[mm.z^{-1}]	a_p[mm]
1	25.12,50.24,75.36,100.48	0.005	0.1
2	50.24	0.005,0.01,0.015,0.02	0.1
3	50.24	0.005	0.005,0.1,0.15,0.2

Tab. 6 *ANOVA results for Ra*

Source of variance	Sum of Squares	Degrees of freedom	Mean square	*F* value	*P* value	
n_s	0.0003	1	0.0003	3.39	0.3235	*
f_z	0.0312	1	0.0312	134.39	0.0014	**
a_p	0.0039	1	0.0039	16.68	0.0265	**
$n_s \times f_z$	0.0001	1	0.0001	0.3112	0.6159	
$n_s \times a_p$	0.0013	1	0.0013	5.74	0.0963	
$f_z \times a_p$	0.0000	1	0.0000	10.51	0.0439	
n_s^2	0.0007	1	0.0007	2.84	0.1907	
f_z^2	0.0006	1	0.0006	2.48	0.2133	
a_p^2	0.0001	1	0.0001	0.3877	0.5777	
ERROR	0.0007	3	0.0002			—
Total	0.0384	12	—	—		—

Tab. 7 *ANOVA results for F*

Source of variance	Sum of Squares	Degrees of freedom	Mean square	*F* value	*P* value	
n_s	13526.84	1	13526.84	97.31	0.0022	**
f_z	2877.37	1	2877.37	20.70	0.0199	*
a_p	3084.27	1	3084.27	22.19	0.0181	*
$n_s \times f_z$	28.20	1	28.20	0.2028	0.6830	
$n_s \times a_p$	56.10	1	56.10	0.4036	0.5704	
$f_z \times a_p$	490.62	1	490.62	3.53	0.1569	
n_s^2	200.36	1	200.36	1.44	0.3161	
f_z^2	758.58	1	758.58	5.46	0.1016	
a_p^2	2371.02	1	2371.02	17.06	0.0258	
ERROR	417.03	3	139.01			—
Total	24751.42	12				—

3 Results and discussions

3.1 Analysis of surface topography and surface roughness

3.1.1 Effect of cutting speed on surface roughness and surface topography

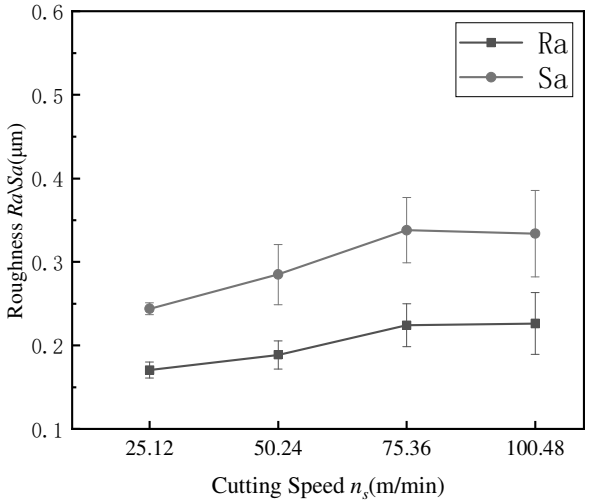

Fig. 3 *Effect of cutting speed on surface roughness*

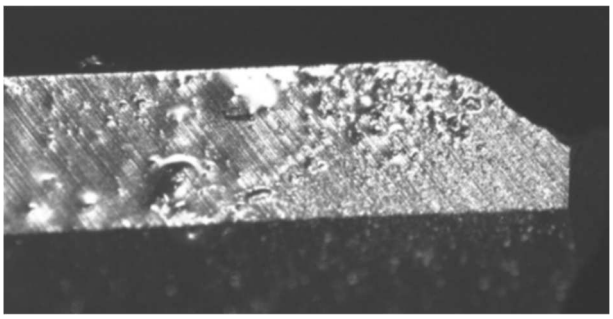

Fig. 4 *Tool wear at n_s = 100.48 m.min^{-1}*

The experimental findings were analysed and processed to get the curves depicting the surface roughness Ra at various cutting speeds. Figures 3 and 5 present the impact of cutting speed on both surface morphology and surface roughness, using the parameters f_z = 0.01 mm.z^{-1} and a_p = 0.1 mm. Based on the data shown in Figure 3, it is evident that the surface roughness values, namely Ra, vary between 0.170 and 0.226 μm, whereas Sa varies from 0.244 to 0.338 μm. The relationship between surface roughness and cutting speed exhibits a non-linear pattern throughout the range of 25.12 to 100.48 m.min^{-1}. The trend of surface roughness exhibits an initial increase followed by a subsequent decrease when the cutting speed is increased. At lower cutting speeds, the emulsion preparation facilitates cooling and lubrication, thereby improving the surface quality of the workpiece. However, increasing the cutting speed from 25.12 to 75.36 m.min^{-1} introduces cutting vibrations caused by the high-speed rotation of the tool. This leads to an increase in cutting force and an unstable machining state, leads to a reduction in the surface integrity of the workpiece. Moreover, the augmentation in cutting forces might induce the extraction of brittle materials, resulting in the emergence of fractures or even depressions on the surface. The presence of many pits on the surface can be attributed to the phenomenon of material extraction. When cutting speed(n_s) is raised from 75.36 to 100.48 m.min^{-1}, there is an observable tendency towards smoother surface morphology, more uniform knife marks, and a modest decrease in surface roughness. There exist two overarching rationales: Firstly, it should be noted that high-speed cutting results in an elevation of temperature, thereby causing a reduction in the hardness of the processed surface, while simultaneously enhancing the plasticity of the

material and increasing fracture toughness. Secondly, the softening of the chips generated during the cutting process leads to a decrease in the friction coefficient, facilitating the removal of metal particles and subsequently contributing to the attainment of a smoother surface roughness. Nevertheless, in cases where the cutting speed is excessively high, there is a rapid increase in the temperature of the machining surface. This can result in accelerated wear of the tool, thereby impeding the advancement of high-speed cutting techniques in the domain of powder metallurgy γ-TiAl alloy machining applications, as depicted in Figure 4. The study conducted by Al-Ahmari et.al.[22]. demonstrated that the ideal process parameters for surface roughness and cutting speed and feed rate are as follows: a cutting speed (n_s) of 87.41 m.min^{-1}, a cutting depth (a_p) of 0.025 mm, and a feed rate (f_z) of 0.3 mm.z^{-1}. Based on the findings depicted in Figure 5, it can be inferred that an escalation in cutting speed correlates with the heightened visibility of surface protrusions, hence resulting in the deterioration of surface morphology.

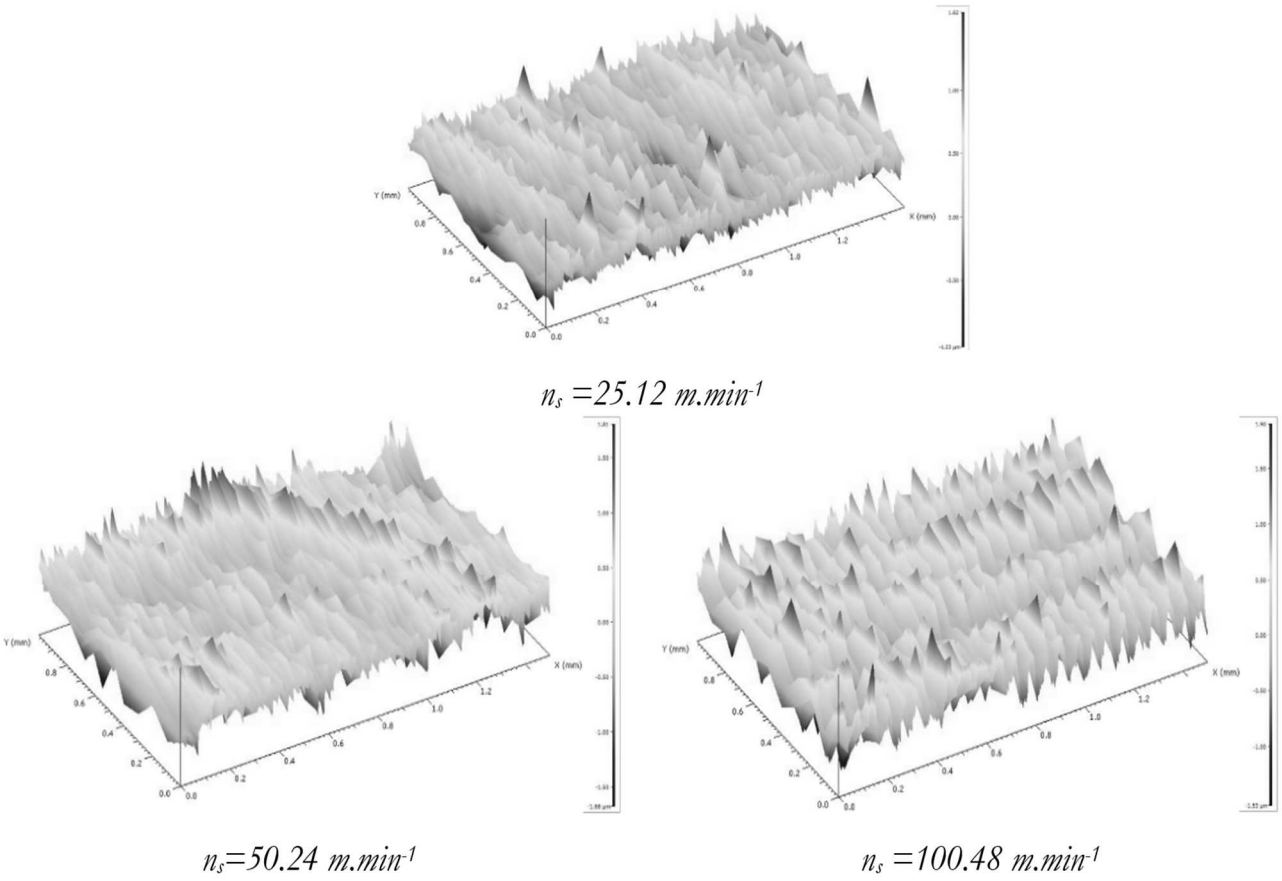

Fig. 5 *The variation trend of surface morphology with cutting speed (a_p=0.1mm and f_z=0.005 mm.z^{-1})*

3.1.2 Influence of cutting depth on surface roughness and surface topography

The trend graph in Figure 6 illustrates the relationship between surface roughness and feed per tooth in the milling process of powder metallurgy γ-TiAl, with a cutting speed(n_s) of 50.24 m.min^{-1} and a feed rate(f_z) of 0.005 mm.z^{-1}. According to the data presented in Figure 6(a), there is an observable linear relationship between the cutting depth and the increase in surface roughness. Furthermore, Figures 6(b) and (c) indicate that as the depth of cut (a_p) is increased from 0.05 mm to 0.25 mm, there is a corresponding increase in the height of the peaks and troughs, resulting in a deterioration of the surface topography. The observed phenomenon can be attributed to the relationship between the cutting depth and various factors affecting the milling process. Specifically, as the depth of cut is increased, there is a corresponding increase in the volume of material being removed per unit time. This increase in material removal leads to greater squeezing and friction between the surface being machined and the cutting tool. Consequently, the resistance encountered during milling is heightened, resulting in amplified machining vibrations. Ultimately, these vibrations contribute to the degradation of the surface quality being produced. However, it is likely that the relatively small selection of cutting speed and feed per tooth have resulted in an inconspicuous changing trend.

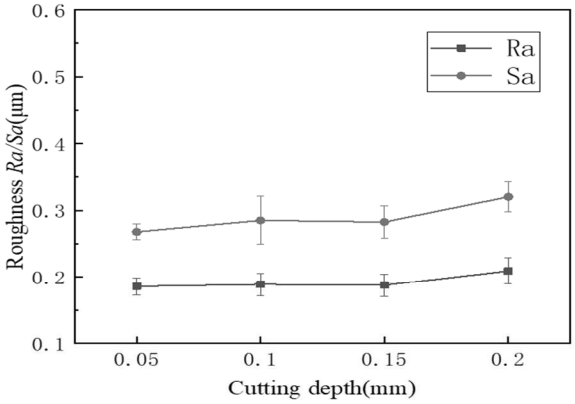

(a) Surface roughness

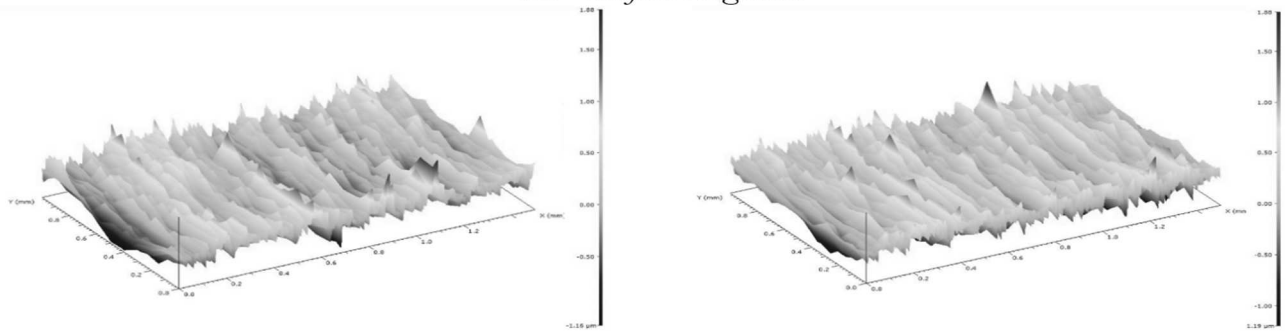

(b) a_p=0.05mm (c) a_p=0.25mm

Fig. 6 *Variation of surface roughness and surface morphology with cutting depth (n_s =50.24 m.min^{-1} and f_z=0.005 mm.z^{-1})*

3.1.3 Influence of feed rate on surface roughness and surface topography

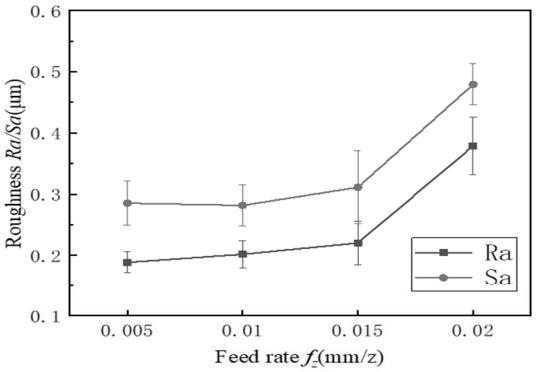

(a) Surface roughness

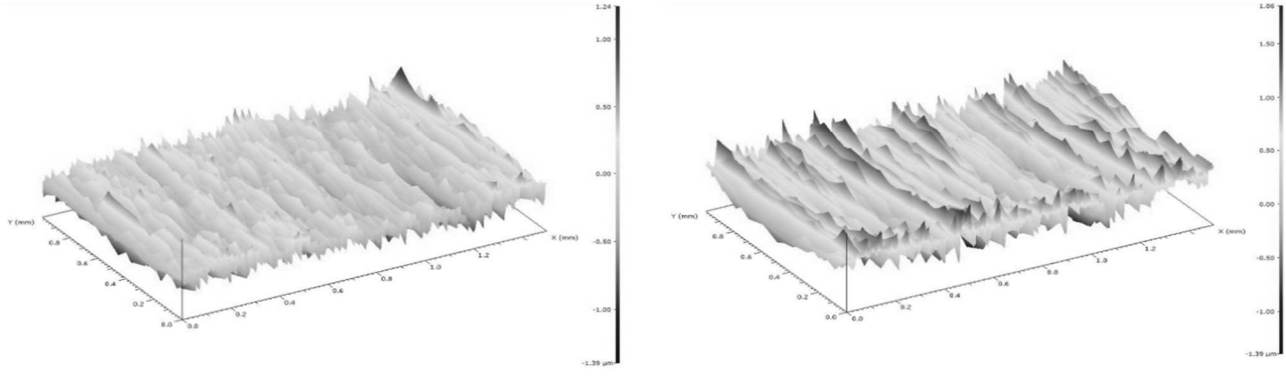

(b) f_z=0.005 mm.z^{-1} (c) f_z=0.02 mm.z^{-1}

Fig. 7 *Variation of surface roughness and surface morphology with feed rate (n_s=50.24 m.min^{-1} and a_p=0.1mm)*

Figure 7 illustrates the surface morphology trend of powder metallurgy γ-TiAl milling, specifically focusing on the variation in feed per tooth. The milling process was conducted at a cutting speed （n_s） of 50.24 m.min^{-1} and an axial depth of cut （a_p） of 0.1 mm. According to the data presented in Figure 7(a), it is evident that the surface roughness exhibits a consistent upward trend as the feed per tooth rises. Additionally, the speed initially demonstrates a rapid increase before transitioning to a slower rate of change. Based on the observations made in Figure 7 (b) and (c), it can be shown that an increase in the feed per tooth f_z from 0. 005 mm.z^{-1} to 0.02 mm.z^{-1} leads to a rise in the number of peaks and valleys on the surface. Additionally, the height of these peaks and valleys becomes steeper, resulting in a progressive deterioration of the surface topography.

3.2 Analysis of cutting force

Figure 8 illustrates the varying trend of the milling force for γ-TiAl alloy in relation to the cutting speed, feed rate, and cutting depth. The cutting force refers to the mean force exerted during a period of steady cutting. Figure 8(a) illustrates the relationship between milling force and cutting speed under the conditions of a_p=0.1mm and f_z=0.005 mm.z^{-1}. Figure 8(a) illustrates that the cutting speed(n_s) ranges from 25.12 to 100.48 m.min^{-1}. Additionally, it is observed that the milling force exhibits a decreasing trend initially, followed by an increasing trend as the cutting speed increases. When the cutting speed is increased from 25.12 to 75.36 m.min^{-1}, there is a drop in the cutting force. Currently, the escalating cutting speed and rising material temperature have resulted in a scenario where the softening effect of the material surpasses the strengthening impact of the material strain rate, leading to a drop in cutting force. Nevertheless, when the cutting speed is raised from 75.36 to 100.48 m.min^{-1}, the impact of elevated temperature on material softening appears to stabilise. However, this increase in cutting speed also exacerbates tool wear during high-speed cutting, resulting in a significant rise in cutting force. Y.F. Ge et al [16] found comparable findings in their investigation of face milling of γ-TiAl, employing identical cutting settings. The cutting force exhibited a reduction as a result of an increase in cutting speed. The observed phenomenon can be attributed to the significant rise in cutting temperature that occurs in tandem with an increase in cutting speed [21]. Currently, the material has a larger propensity for softening compared to the strengthening effect induced by strain. Consequently, the material within the shear zone will undergo a softening process, resulting in a reduction of the cutting force. Hood et al. [15] observed a positive correlation between cutting force and tool wear in the milling process of γ-TiAl. Consequently, while operating at high cutting speeds, the tool experiences accelerated wear, resulting in a pronounced escalation in cutting force.

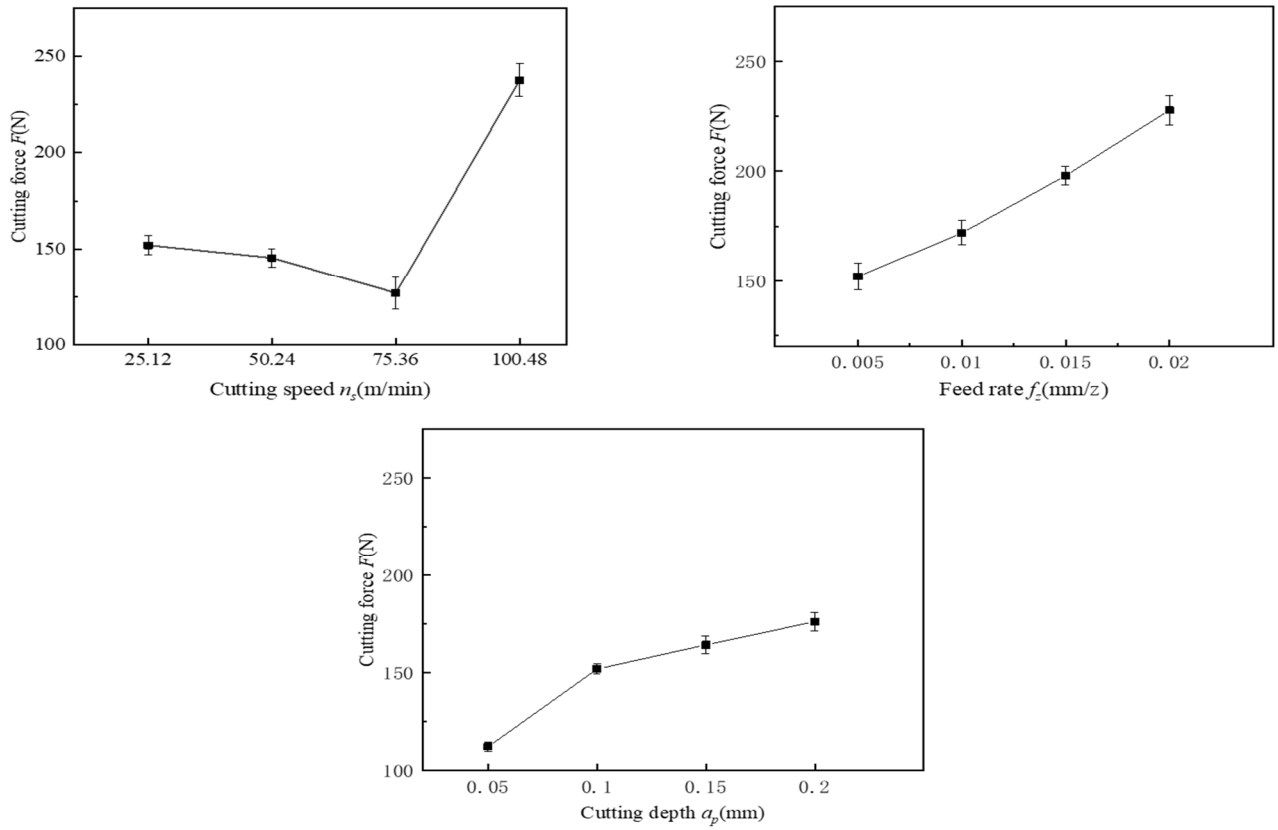

Fig. 8 *Variation of cutting force*

Figure 8(b) demonstrates a noticeable trend wherein the milling force exhibits a nearly linear relationship with the growth in cutting depth, specifically when the cutting speed (n_s) is set at 50.24 m.min^{-1} and the feed speed (f_z) is 0.005 mm.z^{-1}. As the cutting depth was augmented, there was an escalation in the friction occurring between the flank face of the tool and the surface of the work-piece. Consequently, there was an observed amplification in the extrusion occurring between the lamellar layers, resulting in a corresponding augmentation in the material's resistance to deformation. As seen in Figure 8(c), when the cutting speed (n_s) was set at 50.24 m.min^{-1} and the axial depth of cut (a_p) was 0.05 mm, the milling force exhibited a nearly linear relationship with the increment in the feed rate. This phenomenon occurred due to the direct correlation between the feed rate and the amount of material removed with each rotation of the cutter. In contrast, Pérez et al. [23] presented divergent findings in their study on the milling of γ-TiAl (Ti-47Al-2Nb-2 Mn+0.8 vol% TiB_2). The experimental findings indicated that the cutting force attained a magnitude of 700 N under the following cutting conditions: cutting speed (n_s) of 50.87 m.min^{-1}, feed per tooth (f_z) of 0.5 and 0.1 mm, and depth of cut (a_p) of 0.1 mm. Upon comparison, it becomes evident that the disparities mostly stemmed from the cutting parameters, with the cutting force displaying a significant escalation under conditions of substantial cutting depth and feed speed.

3.3 Examination of variation

The empirical findings are shown in Table 4. The analysis of the factorial experiment revealed that the lowest Ra values were seen at a cutting speed of 100.48 m.min^{-1}, a feed rate of 0.005 mm.z^{-1}, and a cutting depth of 0.125 mm. In accordance with the specified experimental parameters, the cutting tests were conducted on two separate occasions. The findings indicated that the surface roughness (Ra) was within the range of 0.24 to 0.406 μm. The accuracy of fitting can be explained by the size of P value in the analysis of variance for the mathematical regression model of surface roughness. In general, a P value less than 0.05 indicates that the model is credible and the better the fitting effect is. The statistical significance of the Ra fitting formula in this study is supported by a P value of less than 0.05, suggesting a high level of significance for the model. It is shown that the mathematical model established in this paper has small error and high reliability and can better reflect the relationship between the surface roughness and the response value and predict the best process parameters.

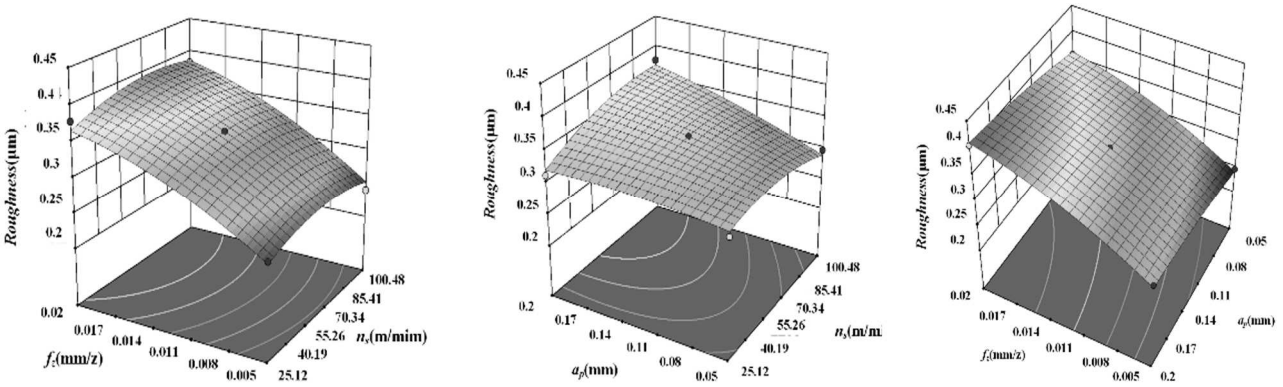

Fig. 9 *Arithmetic mean deviation of profile Ra characteristic surface*

Based on the obtained P value, it can be concluded that the influence of feed rate B and cutting depth C on surface roughness is very significant. Additionally, the interaction term BC exhibits a greater level of significance. However, it is worth noting that the remaining factors do not demonstrate a significant impact, as their P values above the threshold of 0.05. Based on the F value, the hierarchy of effect of three elements on surface roughness is as follows: feed rate holds the greatest influence, followed by cutting depth, and finally cutting speed.

The analysis of variance (ANOVA) findings for Ra are presented in Table 6. The factors that were shown to have a significant impact on the surface roughness (Ra) were the cutting depth, feed rate, cutting speed, and the relationship between cutting depth and cutting speed. The variable that had the highest level of statistical significance in relation to Ra was the feed rate. This variable accounted for 38.71% of the overall variation. The cutting depth accounted for the second highest contribution, comprising 22.38% of the total. Through the Design Expert software, the reaction surface graph and contour graph were constructed to analyze the interplay between several variables and their impact on surface roughness, as shown in Figure 9. The correlation between the cutting depth and feed rate is readily apparent, but the interaction between other factors is not significant. The primary element that significantly affects surface roughness is the feed per tooth, followed by cutting depth, while the cutting

speed has the least discernible impact.

The ANOVA findings for F are presented in Table 7. The significant factors affecting F were determined to be the cutting depth, cutting speed, feed rate, and the interaction between cutting depth and feed rate. The variable that had the greatest statistical significance in relation to F was the cutting depth, which accounted for 34.68% of the overall variation. The cutting speed had the second highest contribution, accounting for 25.78% of the total. Figure 10 displays the response surface and contour diagram illustrating the interaction among several parameters in relation to surface roughness. The correlation between the feed rate per tooth and cutting depth is readily apparent, but the interaction between other factors is not significant. The cutting speed, as a singular element, exerts the most pronounced influence on the cutting force, whereas the cutting depth and feed per tooth exhibit minimal impact on the cutting force. The normal probability plots of residuals for roughness of the surface and force of cutting are illustrated in Figure 11(a) and (b), respectively. The residuals were found to has a high degree of proximity to the fitted regression lines. Therefore, the models may be utilised to forecast the fluctuations in roughness and cutting force throughout the process of milling machining.

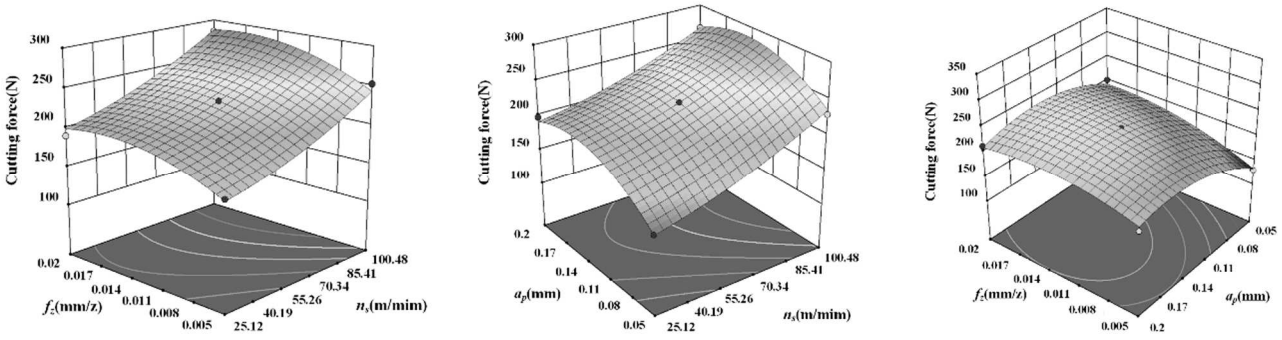

Fig. 10 *Arithmetic mean deviation of profile F characteristic surface*

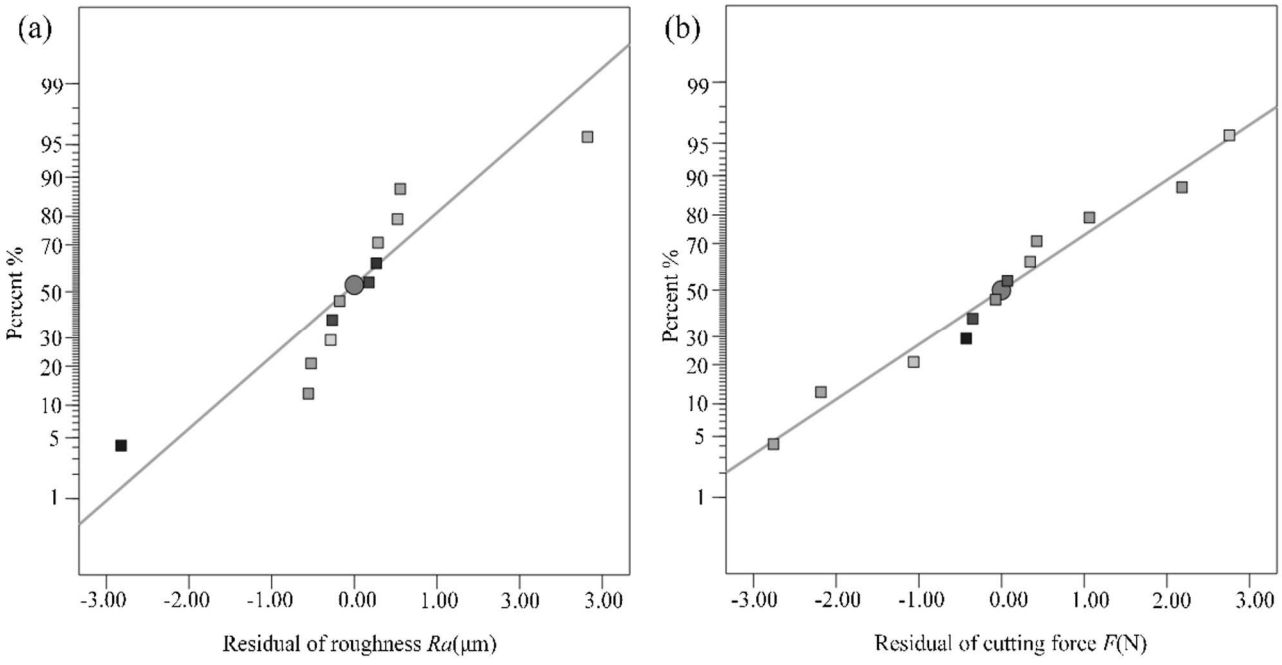

Fig. 11 *Normal probability plots of residual for (a) surface roughness, (b) cutting force*

4 Multi-objective optimization of milling parameters

4.1 Optimization model

The enhancement of cutting quality in powder metallurgy γ-TiAl alloy can be achieved by the reduction of cutting force and surface roughness. Simultaneously, it is necessary to take into account the efficiency of the procedure. The material removal rate (MRR) serves as a valuable metric for evaluating the effectiveness of a processing operation. By enhancing the material removal rate, it is possible to effectively decrease the expenses associated with the processing procedure. The study utilised the NSGA-II non-dominated fast sequencing genetic algorithm to perform

multi-objective optimisation. The inputs included cutting speed, feed rate per tooth, and cutting depth, while the optimisation objectives were surface roughness, cutting force, and material removal rate (MRR). The aim was to obtain the optimal process parameter set that would strike a balance between machining quality and efficiency. The empirical data is shown in Table 8.

Tab. 8 *Experimental data of MRR*

No	n_s [m.min^{-1}]	f_z [mm.z^{-1}]	a_p [mm]	MRR [mm^3.min^{-1}]
1	25.12	0.005	0.125	15
2	25.12	0.02	0.125	60
3	25.12	0.0125	0.05	60
4	25.12	0.0125	0.2	240
5	62.8	0.005	0.05	15
6	62.8	0.02	0.05	60
7	62.8	0.005	0.2	60
8	62.8	0.02	0.2	240
9	62.8	0.0125	0.125	93.75
10	100.48	0.005	0.125	60
11	100.48	0.02	0.125	240
12	100.48	0.0125	0.05	60
13	100.48	0.0125	0.2	240

As indicated in Table 9, multiple linear regression analysis was utilised to create response regression models for cutting force F, surface roughness Ra, and machining parameters, respectively.

Tab. 9 *Linear regression models for Ra and F*

Type	Regression equtions
Roughness	$Ra=0.3462 + 0.00635\ n_s + 0.06245 f_z + 0.022\ a_p + 0.00425\ n_s f_z + 0.01825\ n_s a_p + 0.00235\ f_z a_p - 0.016975\ n_s^2 - 0.015875\ f_z^2 - 0.006275\ a_p^2$
Cutting force	$F=232.65+41.12\ n_s+18.965\ f_z+19.635\ a_p+2.655\ n_s f_z -3.745\ n_s a_p -11.075\ f_z a_p +9.3625\ n_s^2 -18.2175\ f_z^2 -32.2075\ a_p^2$

4.2 Multi-objective optimization via NSGA-Ⅱ

To achieve the desired standards of milling in terms of quality and efficiency, it is imperative to develop a multi-objective optimisation model. This model aims to minimise the surface roughness (Ra) and cutting forces (F), while maximising the material removal rate (MRR). The input variables included in this model are the cutting speed (n_s), feed rate (f_z), and depth of cut (a_p). The goal function and restrictions may be formulated in the following manner:

$$\begin{cases} Min\{Ra(n_s, f_z, a_p)\} \\ Min\{F(n_s, f_z, a_p)\} \\ Min\{-MRR(n_s, f_z, a_p)\} \\ 25.12 \le n_s \le 100.48 \\ 0.005 \le f_z \le 0.02 \\ 0.05 \le a_p \le 0.2 \end{cases} \quad (1)$$

Tab. 10 *Parameters setting in NSGA-Ⅱ*

Parameters	Values
Maximum number of iterations	20
Population size	1000
Crossover percentage	0.8
Mutation percentage	0.1
Mutation rate	0.2

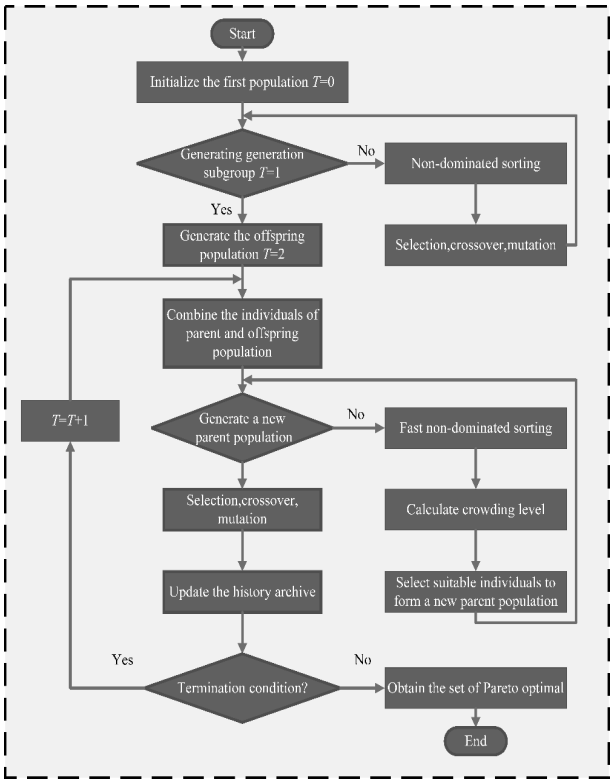

Fig. 12 *The flowchart of multi-objective optimization with NSGA-Ⅱ algorithm*

The NSGA-II method is employed to enhance solution diversity by utilising the crowded comparison operator, which preserves the elitists throughout evolution [24]. This is achieved by sorting the parent population and sub-population. The inclusion of supplementary weight coefficients is unnecessary in instances where the computational workload is reduced. The technique exhibits remarkable stability and flexibility, along with its capability to acquire a Pareto optimal solution set that is evenly distributed. The regression models (Ra, F) are optimised using the NSGA-II algorithm, resulting in the identification of the Pareto optimum solution. Figure 12 depicts the flow chart of NSGA-II. The first input comprises the goal function and a set of restrictions. Furthermore, the genetic operators accountable for the processes of crossover and mutation give rise to a novel population. Subsequently, the use of the elite technique is employed to safeguard the superior portion of the recently produced populace with each iteration. The optimisation procedure is computed based on the amount of repeats, as shown by previous research [25].

The NSGA-Ⅱ algorithm's ability to get the Pareto optimal solution set is directly impacted by two factors: the population size (k) and the number of iterations (T) [26]. In order to improve the accuracy of the calculation, it is crucial to carefully choose the parameters for the multi-objective optimisation technique. Within the framework of the algorithm's execution, the population size is denoted as k=1000. The probability of identifying a global solution increases as the population size grows greater. Nevertheless, the computational efficiency of this approach will be diminished. Table 10 displays the pertinent parameters utilised in NSGA-Ⅱ. Figure 13 illustrates the alteration in the distribution of Pareto-optimal solutions as the number of iterations increases, ranging from T=0 to T=20. As seen in Figure 13(c), the population distribution exhibits a notable concentration as the iteration progresses to T=20. The results suggest that the value of T=20 meets the requirements for optimisation.

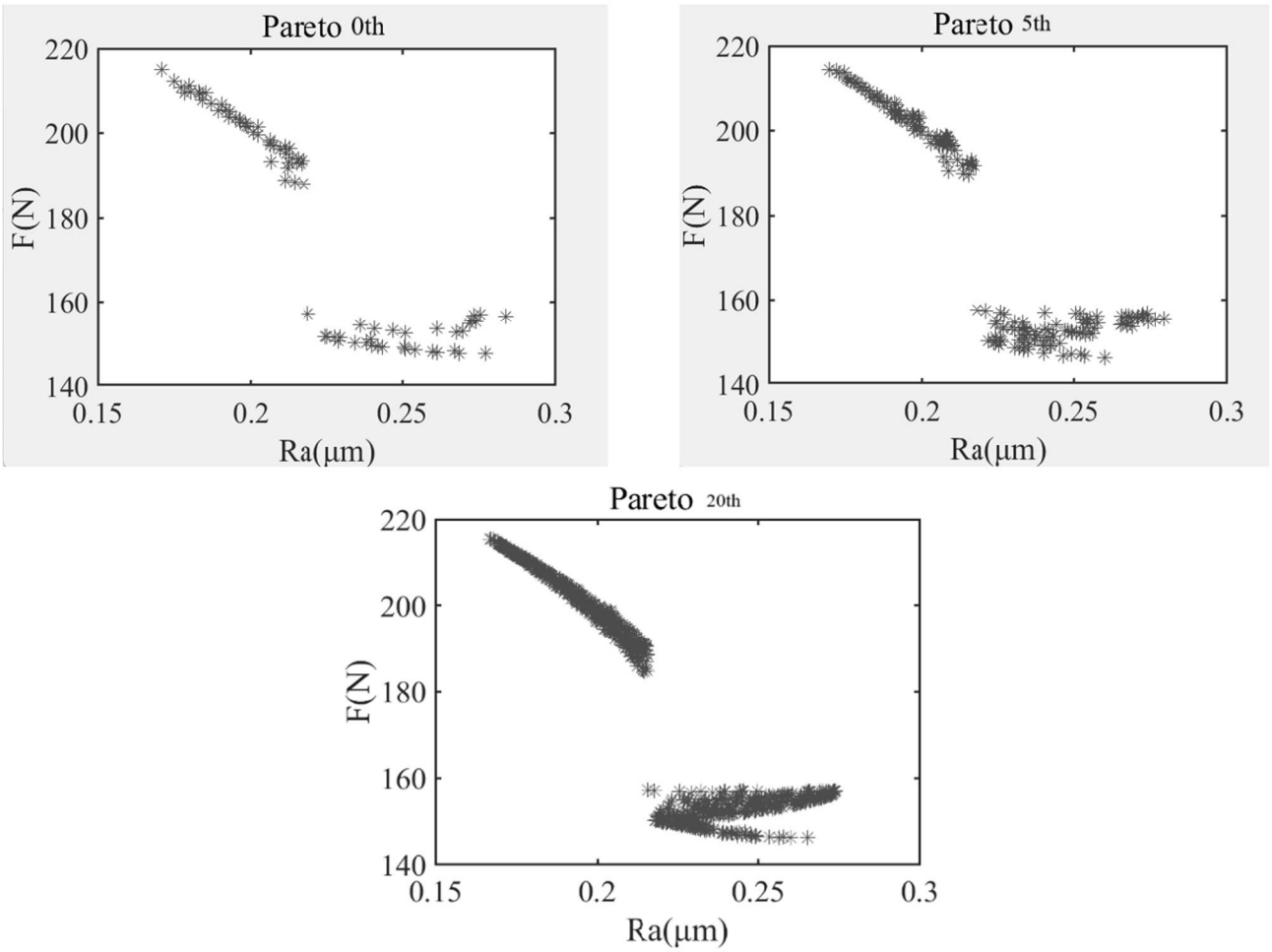

Fig. 13 *The distribution of Pareto-optimal solutions in NSGA-Ⅱ with k=2000 at (a) T=0, (b) T=5, (c) T=20.*

Table 11 presents a selection of five sets of machining parameters that exhibit the largest congestion. These sets are chosen as representations in the projection of optimal solutions on each plane of response variables.

Tab. 11 *Multi-objective optimum set of machining parameters for milling*

No	n_s [m.min^{-1}]	f_z[mm.z^{-1}]	a_p [mm]	F [N]	R_a [μm]	MRR [mm^3.min^{-1}]
1	91.56	0.0062	0.083	206.8	0.233	54.810
2	67.40	0.0125	0.075	163.89	0.238	58.424
3	82.12	0.0081	0.160	198.63	0.279	66.506
4	55.46	0.0062	0.052	154.62	0.204	18.772
5	36.62	0.0162	0.193	188.62	0.323	31.440

4.3 Optimization results and confirmation parameters

Conduct experimental verification according to the optimized parameter combination in the previous section (due to practical factors, the feed speed and cutting depth are rounded). Measure the roughness of surface and force of cut of the test block, and calculate the predicted values based on the model. Compare the two to obtain the error of surface roughness and cutting force, as shown in Table 12. Under the five sets of process parameters, The mean relative error among the experimentally determined and anticipated values of roughness of the surface is 0.13%, whereas the mean relative error among the experimentally determined and forecasted values of the cutting force is 8.35%. This indicates that the model can effectively predict cutting force and surface roughness, indicating milling processing γ- The correctness of the optimal process parameters for TiAl alloy.

Tab. 12 *Experimental results of confirmation tests*

No	n_s [m.min^{-1}]	f_z [mm.z^{-1}]	a_p [mm]	F		Ra [μm]	
				Actual value	Error	Actual value	Error
1	91.56	0.0062	0.083	223.6	8.1%	0.258	9.17%
2	67.40	0.0125	0.075	165.7	1.7%	0.256	8.7%
3	82.12	0.0081	0.160	178.6	11.2%	0.288	3.12%
4	55.46	0.0062	0.052	165.9	7.1%	0.221	7.6%
5	36.62	0.0162	0.193	195.1	3.3%	0.352	8.14%

Among the 5 optimal parameter combinations, the surface roughness of No. 1 is relatively small, but the cutting force is relatively high, which is easy to cause tool vibration; The machining efficiency of No. 3 is relatively high; However, it is observed that the surface roughness and cutting force exhibit comparatively high values. The fourth cutting force has the lowest magnitude, while concurrently yielding the most favourable surface roughness.， but the processing efficiency is the lowest and the processing time is the longest; The machining efficiency of No. 5 is relatively high, but the surface roughness is the highest. Due to the hard and brittle nature of the material, the cutting force exerts a substantial influence on the stability of the workpiece., and the cutting force F should not be too large. Therefore, priority should be given to selecting No. 2 and No. 4. Additionally, as the machining efficiency of No. 2 is much higher than that of No. 4, No. 2 is chosen as the optimal parameter combination.

5 Conclusions

The limitation of the widespread application of powder metallurgy γ-TiAl alloys in aerospace and other sectors is mostly attributed to the surface integrity. This research presents a systematic analysis of the impact of cutting parameters on the surface integrity of powder metallurgy γ-TiAl alloys. Single-factor tests were conducted to investigate this influence. The findings of this study can be summarised as follows:

- (1) The analysis of the factorial experiment revealed that the lowest Ra values were achieved at n_s= 25.12 m.min^{-1}, f_z = 0.005 mm.z^{-1}, and a_p = 0.1 mm. In accordance with the specified experimental parameters, the cutting experiments were replicated twice. The Ra value fell within the range of 0.17 to 0.379 μm.
- (2) The surface quality of powder metallurgy γ-TiAl alloys processing exhibits a decline as the cutting depth and feed rate rise, as well as with an increase in cutting speed, but it will slightly improve after reaching a certain value. Within the range of cutting speed ns increasing from 25.12 to 75.36 m.min^{-1}, the surface roughness value increases with the increase of cutting speed ns. After the cutting speed ns reaches 75.36 m.min^{-1}, it actually decreases with the increase of cutting speed ns, but tool wear will sharply increase. It is recommended to select a larger cutting speed during milling and reduce the feed rate and

cutting depth without affecting the processing efficiency.

- (3) The feed rate is identified as the primary determinant influencing the surface shape of machined powder metallurgy γ-TiAl alloys. The machined surface quality is inversely proportional to the increase in feed rate and cutting depth. The cutting force of powder metallurgy γ-TiAl alloys is primarily influenced by the cutting speed. Additionally, the interplay between the feed rate per tooth and the cutting depth also exerts a discernible effect on the cutting force.
- (4) Analyze the optimization results, select representative optimization solutions from all optimization results, and then conduct experimental verification. The experimental results indicate that the error between the experimental and predicted values does not exceed 10%, indicating the accuracy and reliability of the model and optimization results under certain conditions. Finally, a set of comprehensively optimal parameter combinations was selected in the optimization solution. In this paper, n_s=67.4 (m.min^{-1}), f_z=0.0125 (mm.z^{-1}), and a_p=0.075 (mm) were selected as the optimal machining parameters for powder metallurgy γ- TiAl alloys milling processing.

Author contributions

All authors contributed to the study conception and design. Material preparation, data collection, and analysis were performed by Wenbing Tian. The first draft of the manuscript was written by Wenbing Tian and all authors commented on previous versions of the manuscript. All authors read and approved the final manuscript.

Acknowledgement

This article is supported by the project "Research on TiAl-4522XD Alloys Low Pressure Turbine Working Blade Powder Hot Isostatic Pressing Near Net Forming Technology" hosted by China Aviation Industry Corporation, with project number ZZCX-2020-007.

References

[1] CHEN G, PENG Y, ZHENG G, ET al. Polysynthetic twinned TiAl single crystals for high-temperature applications. *Nat Mater* 2016; 15:876–81.

[2] LORIA EA. Gamma titanium aluminides as prospective structural materials. *Intermetallics* 2000; 8(9–11): 1339–45.

[3] LORIA EA. Quo vadis gamma titanium aluminide. *Intermetallics* 2001; 9(12): 997–1001.

[4] YAO C, LIN J, WU D, et al. Surface integrity and fatigue behavior when turning γ-TiAl alloy with optimized PVD-coated carbide inserts. *Chin J Aeronaut* 2018; 31(4): 826–36.

[5] KUNAL KOTHARI, RAMACHANDRAN; NORMAN M. WERELEY. Advances in gamma titanium aluminides and their manufacturing techniques[J]. *Progress in aerospace sciences*, 2012, 55(Nov.):1-16.

[6] ZHANG X Y, LI C W, ZHENG M Y,ET al. Chemical, microstructure and mechanical property of TiAl alloys produced by high-power direct laser deposition [J]. *Journal of Materials Science & Technology*, 2022, 117: 99-108.

[7] PRIARONE PC, RIZZUTI S, SETTINERI L, et al. Effects of cutting angle, edge preparation, and nano-structured coating on milling performance of a gamma titanium aluminide. *J Mater Process Technol* 2012;212(12):2619–28.

[8] PAOLO C. PRIARONE, MATTEO ROBIGLIO, LUCA SETTINERI, et al. Milling and turning of titanium aluminides by using minimum quantity lubrication[C]. *Procedia CIRP2014*,Pages 62-67, ISSN 2212-8271,

[9] KOLAHDOUZ S, AREZOO B, HADI M. Surface integrity in high-speed milling of gamma titanium aluminide under MQL cutting conditions. *Thermal power plants*. IEEE; 2015. p. 62–9.

[10] ROTELLA G, PRIARONE PC, RIZZUTI S, et al. Evaluation of the environmental impact of different lubrorefrigeration conditions in milling of γ-TiAl alloy. *Glocalized solutions for sustainability in manufacturing*. Berlin Heidelberg: Springer; 2011. p. 365–70.

[11] LUCA SETTINERI, PAOLO C. PRIARONE, MARTIN ARFT, et al. An evaluative approach to correlate machinability, microstructures, and material properties of gamma titanium aluminides[J]. *CIRP Annals*,2014,63(1 CD/ROM):57-60.

[12] BERANOAGIRRE, A., OLVERA, D., LÓPEZ DE LACALLE, L.N., 2012, Milling of gamma titanium-aluminum alloys. *Int J Adv Manuf Technol*, 62:83–88.

[13] HOOD, R., ASPINWALL, D.K., SOO, S.L., MANTLE, A.L., NOVOVIC, D., 2014, Workpiece surface integrity when slot milling g-TiAl intermetallic alloy. *CIRP Ann Manuf Technol*, 63:53–56.

[14] MANTLE, A.L., ASPINWALL, D.K., 1997, Surface integrity and fatigue life of turned gamma titanium aluminide. *J Mater Process Technol*, 72:413–420.

[15] HOOD R, ASPINWALL DK, Sage C, et al. High speed ball nose end milling of γ-TiAl alloys. *Intermetallics* 2013;32:284–91.

[16] Y.F. GE, Y.C. FU, J.H. XU. Experimental Study on High Speed Milling of Y-TiAl Alloy[C]. *Progress of Precision Engineering and Nano Technology*. 2007.

[17] ARIF M, RAHMAN M, SAN WY. Analytical model to determine the critical conditions for the modes of material removal in the milling process of brittle material. *J Mater Process Technol* 2012;212(9):1925–33.

[18] ZHANG X, ARIF M, LIU K, et al. A model to predict the critical undeformed chip thickness in vibration-assisted machining of brittle materials. *Int J Mach Tools Manuf* 2013;69(3):57–66.

[19] XIAO Y, CHEN MJ, YANG YT, et al. Research on the critical condition of brittle-ductile transition about micro-milling of KDP crystal and experimental verification. *Int J Precis Eng Manuf* 2015;16(2):351–9.

[20] ASPINWALL DK, DEWES RC, Mantle AL. The machining of γ-TiAl intermetallic alloys. *CIRP Ann–Manuf Technol* 2005;54:99–104.

[21] ASPINWALL DK, MANTLE AL, CHAN WK, et al. Cutting temperatures when ball nose end milling γ-TiAl intermetallic alloys. *CIRP Ann–Manuf Technol* 2013;62(1):75–8.

[22] AL-AHMARI A, ASHFAQ M, ALFAIFY A, et al. Predicting surface quality of γ-TiAl produced by additive manufacturing process using response surface method[J]. *Journal of Mechanical Science and Technology*,2016,30(1).

[23] PÉREZ RGV. Wear mechanisms of WC inserts in face milling of gamma titanium aluminides. *Wear* 2005;259(7):1160–7.

[24] X. CHEN, B. JIANG, Z. ZHOU, Optimization of CFRP pultrusion process with NSGA-II and ANN, *Adv. Mater. Res.* 538–541 (2012) 2705–2711.

[25] J. LI, W. ZUO, J. E, Y. ZHANG, Q. LI, K. SUN, K. ZHOU, G. ZHANG, Multi-objective optimization of mini U-channel cold plate with SiO2 nanofluid by RSM and NSGA-II, *Energy.* 242 (2022) 123039.

[26] Q. WANG, X. JIA, Multi-objective optimization of CFRP drilling parameters with a hybrid method integrating the ANN, NSGA-II and fuzzy C-means, *Compos. Struct.* 235 (2020) 111803.